Analyst

Accepted Manuscript

ROYAL SOCIETY OF CHEMISTRY

www.rsc.org/analyst

Cite this: DOI: 10.1039/c0xx00000x

www.rsc.org/xxxxxx

ARTICLE TYPE

Development of a Particle-Settling Tolerant Transmission Raman Scheme for Analysis of Suspension Samples

Kayeong Shin[a], Pham Khac Duy[a], Sijun Park[a], Young-Ah Woo[b] and Hoeil Chung[a]*

Received (in XXX, XXX) Xth XXXXXXXXX 20XX, Accepted Xth XXXXXXXXX 20XX

DOI: 10.1039/b000000x

We have demonstrated a simple and effective strategy, a so-called axial illumination scheme, that is able to obtain representative Raman spectra of suspension samples with minimal influence from internal particle settling. In a partially settled suspension sample, since particle concentrations at given points throughout the sample differ, the acquisition of Raman spectra representative of the entire sample composition is critically important for accurate quantitative analysis. The proposed scheme used axially irradiated laser radiation in the same or opposite direction of settling, thus allowing laser photons to migrate through the settling-induced particle-density gradient formed in the suspension and to widely interact with particles regardless of their settled location. Therefore, transmitted Raman signals gathered opposite the illumination could be more representative of the overall suspension composition even with partial settling. In this study, the performance of axial illumination schemes (TB (Top-to-Bottom) and BT (Bottom-to-Top) illumination) was evaluated for the determination of aceclofenac (a non-steroidal anti-inflammatory drug) concentration in suspensions. Although the spectral features exhibited minute variation during settling, settling did not significantly degrade the accuracy of the concentration determination, thereby indicating effective acquisition of settling-tolerant Raman spectra. In addition, the characteristics of photon migration in a partially-settled suspension sample were studied with a simulation based Monte-Carlo method.

Introduction

A suspension is a solution containing suspended solid particles with desired chemical functionality, which is widely utilized in diverse fields, in particular in the manufacture of pharmaceuticals.[1-6] A pharmaceutical suspension is mostly a turbid mixture of an active pharmaceutical ingredient (API) with a supporting syrup matrix. When either back-scattering or

Cite this: DOI: 10.1039/c0xx00000x

www.rsc.org/xxxxxx

ARTICLE TYPE

transmission Raman schemes are employed to analyze a suspension sample, the settling of particles during measurement is a major concern for quantitative analysis. Even in a transmission scheme with laser irradiation perpendicular to the direction of settling on the lower part of a sample, the acquired Raman spectrum will more heavily feature settled denser particles, thus not accurately representing the overall composition of the suspension. Although particles do not quickly precipitate in a viscous solution, even minute and visibly unrecognizable settling could result in non-representative Raman spectra and could adversely influence the accuracy of the concentration determination. Stirring a suspension solution during spectral acquisition would be one possible way to avoid the collection of non-representative spectra; however, spectral reproducibility would be further influenced by additional factors such as stirring rate and swirling.[2] Moreover, for non-destructive analysis of a suspension, sample stirring is not applicable. Therefore, a strategy for acquiring representative Raman spectra of a suspension sample even under ongoing particle settling is highly demanding.

Here, we first demonstrate a simple and effective strategy to obtain settling-tolerant Raman spectra of suspension samples. The method uses a transmission spectral collection scheme in which the sample is axially illuminated with laser radiation in the same or opposite direction of particle settling, allowing laser photons to migrate through the settling-induced particle-density gradient formed in the suspension and widely interacting with particles regardless of their settled locations. The obtained transmitted Raman features are more representative of the overall suspension composition even in the occurrence of partial settling. For an evaluation of this method, suspensions of aceclofenac (a non-steroidal anti-inflammatory drug)[7] with different concentrations were prepared, and concentration determinations were attempted using the proposed axial illumination scheme.

Initially, laser illumination of the sample was perpendicular with respect to settling direction, and Raman spectra were continuously collected during settling at the upper and lower areas of a glass vial containing the aceclofenac suspension. Variations of spectral features at these locations were examined as a function of settling time. Next, transmission Raman spectra of the same samples were collected using the axial illumination scheme in which the laser irradiation was projected in the same and opposite directions of the settling, referred to as the Top-to-Bottom (TB) and Bottom-to-Top (BT) schemes, respectively. Variations of spectral features acquired by both schemes during settling were examined and compared. The characteristics of photon migration in both schemes was expected to be dissimilar, since laser photons in the TB and BT schemes initially interact with particles in relatively less dense and more dense environments, respectively, as settling occurs.

Cite this: DOI: 10.1039/c0xx00000x

www.rsc.org/xxxxxx

ARTICLE TYPE

To determine the aceclofenac concentration, a partial least squares (PLS) model was developed using spectra collected under conditions of homogeneous particle distribution, and the developed model was used to predict aceclofenac concentrations as settling proceeded in the samples. If there were minimal or no influence of settling on the transmission spectral features, the prediction accuracy would not be significantly degraded. Finally, to understand the characteristics of photon migration in the TB and BT schemes, a simulation based on the Monte-Carlo method was performed. For the simulation, a suspension solution was horizontally divided into 8 layers, and the number of particles in each layer was gradually varied to generate a particle-density gradient that mimicked particle settling. Then, photons were axially injected either from the top or bottom through the 8-layered suspension, and the occurrence of Raman photons in each layer were evaluated for both schemes.

Experimental

Preparation of aceclofenac suspensions

An appropriate amount of aceclofenac powder, 2-[[2-[2-[(2,6-dichlorophenyl)amino]phenyl]acetyl]oxy] acetic acid, was added in thoroughly melted excipient solutions at 60 °C, and turbid suspensions were completely homogenized. The amount of aceclofenac varied from 70 to 130 mg with intervals of 3 mg in a 260 mg pure suspension solution. The concentration for each suspension was expressed as the percentage relative to 100 mg, the target dosage in an aceclofenac suspension. For example, suspension samples containing 70 and 130 mg of aceclofenac were designated as 70 % and 130 %, respectively. All of the samples for this study were prepared by a Korean pharmaceutical company. The suspension samples were thoroughly vortexed over one minute when sample homogeneity was necessary for measurement. Figure 1 (a) shows photographs of the 70%, 100%, and 130% aceclofenac suspensions in glass vials. These samples were very hazy, and the 130% aceclofenac sample was slightly more turbid.

Instrumentation, multivariate analysis, and Monte-Carlo simulation

Transmission Raman spectra were collected by directly illuminating laser radiation (785 nm, Invictus, Kaiser Optical Inc.) on a sample, and the transmitted Raman signal was collected in the opposite direction from laser illumination using a wide area illumination (WAI) scheme (PhAT system, Kaiser Optical Inc., Ann Arbor, MI, USA).[8] The diameter of the laser illumination spot was approximately 1.5 mm, and the laser power at the sample was approximately 200 mW. The

Cite this: DOI: 10.1039/c0xx00000x

www.rsc.org/xxxxxx

ARTICLE TYPE

resolution of collected spectra was 4 cm^{-1}. Fifty Raman spectra were continuously collected during a one-hour settling period. Each spectrum was acquired over 30 seconds (exposure time: 3 s, 10 scans) and a subsequent spectrum was collected after 40 seconds of delay. Transmission Raman spectra of aceclofenac samples were obtained using a custom-made aluminum cell, a cylindrical cell (outer diameter: 35.1 mm, inner diameter: 18.0 mm, thickness: 8.0 mm) covered with quartz windows (thickness: 1.25 mm, Hellma Analytics, Germany) at top and bottom of the cell.

All spectral processing and multivariate analyses, including baseline correction, intensity normalization, and PLS, were conducted using MATLAB version 7.0 (The Math-Works Inc., MA, USA). A Monte-Carlo simulation was performed using Montcarl Version 2013, a free computational package.[9,10]

Results and Discussion

Raman spectral features of aceclofenac suspension with perpendicular laser illumination

Fig. 1 (b) shows Raman spectra in the 1800-200 cm^{-1} range of the 100% aceclofenac suspension (red), pure aceclofenac powder (black) and neat suspension solution (blue) samples. After vigorous vortexing to ensure homogeneity of particle distribution, transmission Raman spectra were immediately collected with perpendicular laser illumination of the sample as graphically presented in Figure 2 (a). The wavy and straight arrows indicate the direction of laser illumination and settling (gravitation), respectively. Many distinct peaks corresponding to aceclofenac were present across the spectral range (Fig. 1 (b)), while relatively few peaks with broad features were observed for the neat suspension solution. As expected, the spectrum of the 100 % aceclofenac suspension contained combined spectral information from both pure aceclofenac powder and the neat suspension solution. For further spectral examination and determination of aceclofenac concentration, the 1800-1400 cm^{-1} range was solely used since the aceclofenac bands were the most intense in this region, including the strongest peak at 1589 cm^{-1} (marked by an asterisk in Fig. 1 (b)), and did not severely overlap with bands from the pure suspension solution.

In the case of perpendicular illumination, the settling of aceclofenac particles obviously altered the particle population in a sampled volume for Raman spectral acquisition; thus, Raman intensities of both the aceclofenac and suspension solution bands were not consistent during settling. For the investigation, laser radiation perpendicularly illuminated the upper (#1 position) and lower (#2 position) areas of a suspension sample as described in Fig. 2 (a), and 50 transmission Raman

Cite this: DOI: 10.1039/c0xx00000x

www.rsc.org/xxxxxx

ARTICLE TYPE

spectra were continuously collected over a one hour settling period.

Figure 3 (a) shows normalized Raman spectra of the 100 % aceclofenac sample collected at the 1st, 25th, and 50th snapshots from perpendicular laser illumination of the upper (blue) and lower (red) areas of the sample. The spectra collected by upper area illumination are arbitrarily offset for comparison. For normalization, the baselines of raw spectra were linearly corrected at 1800, 1708, 1627, 1550, and 1400 cm^{-1}, and baseline-corrected spectra were divided by the corresponding peak area under the 1800-1400 cm^{-1} range. For detailed examination, major aceclofenac and suspension solution peaks at 1589 (marked by asterisk) and 1665 cm^{-1} (marked by star), respectively, are highlighted as shown in Figure 3 (b). The arrows indicate the direction of intensity change with settling. As expected, with upper area illumination, intensities of the aceclofenac and suspension solution bands synchronously decreased and increased, respectively, with settling. Exactly the reverse trend in intensity variation was observed with the lower area illumination measurement. It is obvious that the particle density in the sampled volume continuously varied with settling and was denser in the lower area. Since the rate of settling is influenced by particle density in a suspension, the degree of intensity variation could vary depending on the aceclofenac concentration. To examine this effect, three samples of 70 %, 100 % and 130 % aceclofenac were selected, and their intensity variations at 1589 cm^{-1} (aceclofenac) were monitored. Figure 4 shows the intensity variation of aceclofenac bands during a one hour settling period obtained from the 70 % (red), 100 % (blue) and 130 % (black) samples with upper (filled square) or lower area (open square) illumination. The intensity variation for the 130 % aceclofenac sample is magnified in the inset. For the upper area illumination, the intensities in the 70 % and 100 % aceclofenac samples decreased as expected; however, the decrease was much steeper for the 70 % aceclofenac sample. Meanwhile, the intensity variation was minimal for the 130 % aceclofenac sample. Obviously, settling was faster for samples of lower concentration. The trend of intensity variation was exactly the reverse of the lower area illumination measurement.

The intensity variations during settling were quantitatively compared. A linear regression was performed for snapshot number vs. intensity (data in Fig. 4), and the percent variation of intensity at the 50th snapshot relative to the 1st snapshot based on the derived regression line was calculated as shown in Table 1. The calculated percentage over 100 % in the table implies that the intensity at the 50th snapshot increased compared to that at the 1st snapshot. For the 70 % and 100 % aceclofenac samples, intensity variations were larger with upper area illumination compared to lower area illumination. The intensity variations for the 130 % aceclofenac sample were insignificant in both cases.

Cite this: DOI: 10.1039/c0xx00000x

www.rsc.org/xxxxxx

ARTICLE TYPE

To explain the observed difference in intensity variation, it is valuable to understand the factors that affect settling velocity. It is known that settling velocity is related to the type of settling, which depends on the concentration of particles in a suspension solution.[11] When particles are sparsely distributed (low particle concentration), free settling in which individual particles independently settle without interference from surrounding particles occurs. In contrast, when particles are crowded, such as for a particle concentration greater than 20 g/L, surrounding particles interfere with the motion of individual particles and hindered settling takes place.[12] Since the particle concentration of the 70 % aceclofenac sample is equivalent to 304.4 g/L, hindered settling occurred for all samples used in this study.

McGhee's equation describes the velocity of settling for spherical particles under hindered settling conditions as shown below;[13-15]

$$V_h = (1 - C_v)^{4.65} \cdot V_f \qquad \text{(Equation 1)}$$

Where V_h, V_f, and C_v are the hindered settling velocity, free settling velocity, and volume fraction of solid particles in a suspension. C_v was calculated using the known volumes of aceclofenac powder and pure suspension solution in the sample preparation. For the calculation of V_f, aceclofenac particles were assumed to be spherical with a diameter of 20 μm, an approximate average particle size based on the particle size distribution determined by calculating the sizes of 7000 randomly selected dispersed particles in optical images using an image analysis program (Image J, National Institutes of Health, USA). Then, equation (2) based on Stokes' law describing free settling was used as shown below;[16]

$$V_f = \frac{d^2 g\,(e_s - e_w)}{18\mu} = kd^2 \qquad \text{(Equation 2)}$$

where d, g, e_s, e_w, and μ are the particle size (20 μm), acceleration of gravity (9.8 m/s^2), density of aceclofenac powder (1.455 g/cm^3), density of suspension solution (1.128 g/cm^3), and viscosity of solution (1.0152 g/cm·s), respectively. The calculated V_f was 0.7015 μm/s.

Figure 5 shows the variation of hindered settling velocity (V_h) as a function of solid volume fraction (C_v). C_v of 0.40 and

Cite this: DOI: 10.1039/c0xx00000x

www.rsc.org/xxxxxx

ARTICLE TYPE

0.57 corresponds to an aceclofenac concentration of 70 % and 130 %, respectively, as indicated by the dashed lines. As shown, the relationship is not linear, and V_h is faster as C_v becomes lower, such as in the upper area of the 70 % aceclofenac sample. Using the same rationale, settling is progressively slower in the lower area of the sample. Hindered settling explains the steeper decrease of aceclofenac intensity in the upper area and relatively less steep intensity change in the lower area during settling as observed in Fig. 4.

Raman spectral features of aceclofenac suspension with axial laser illumination

As proposed, the TB and BT schemes described in Fig. 2 (b) and (c), respectively, allow photons to migrate axially through the suspension, such that the sampling volume for Raman spectral collection would greatly increase and the acquired spectrum would be more composition representative with much less influence from settling. Figure 6 (a) shows the baseline-corrected Raman spectra of the 100 % aceclofenac sample in the 1800-1400 cm^{-1} range collected by the TB (blue) and BT (red) schemes. The thickness (axial distance across the sample) of aceclofenac suspension samples was 8 mm, the mimicked size of a suspension -containing pharmaceutical capsule. Raman spectra collected at the 1^{st}, 25^{th} and 50^{th} snapshots are displayed for both cases. Spectra collected using the TB scheme are arbitrarily offset for easy spectral comparison. Both aceclofenac (asterisk) and neat suspension (star) bands are magnified on the top. In both cases, the Raman intensities of these two bands decreased slightly with settling. The decreased Raman intensity could primarily occur from attenuation of Raman photons in a section of denser particle population formed by settling. It is important to point out that the decreases of both the aceclofenac and suspension solutions were synchronous, unlike the see-saw type variation observed with perpendicular illumination (see Fig. 3 (b)). Fig. 6 (b) shows normalized Raman spectra corresponding to the baseline-corrected spectra shown in Fig. 6 (a). Again, both aceclofenac (asterisk) and neat suspension (star) bands are magnified on the top. After normalization, the spectral features collected at the 1^{st}, 25^{th} and 50^{th} snapshots were nearly identical. This result indicates that the axial illumination schemes enable Raman spectra to be acquired with superior compositional representation of the entire suspension sample even with the occurrence of partial settling.

Variations in the intensity of the aceclofenac band for the same three samples were also investigated. Figure 7 shows the intensity variation of the normalized aceclofenac band during one hour settling for the 70 % (red), 100 % (blue), and 130 % (black) samples using the TB (filled circle) and BT (open circle) measurements. It is important to note that the magnitude of the *y*-scale is the same as that shown in Fig. 4. For detailed examination, the variations for each case are magnified in the

Cite this: DOI: 10.1039/c0xx00000x

www.rsc.org/xxxxxx

ARTICLE TYPE

insets. At a glance, the intensities are nearly steady over the one hour period of settling.

As similarly calculated in Table 1, the percent variation of intensity at the 50th snapshot relative to the 1st snapshot is shown in Table 2. For all three samples, there was no significant variation in the intensity of the aceclofenac band, demonstrating the settling-tolerant sampling ability of the axial illumination schemes. Meanwhile, there was a subtle difference in the intensity fluctuation between the schemes as observable in the insets. For quantitative evaluation, relative standard deviations (RSDs) of 50 intensity values were calculated for each sample. The numbers in parentheses in the table indicate the resulting RSDs. For each sample, the RSD was slightly higher for the BT measurement compared with the TB measurement. It appears that initial laser illumination on a denser part of the suspension (BT scheme) increases the uncertainty in photon propagation through a partially settled sample.

Monte-Carlo simulation to study Raman photon distribution in a suspension sample

To further characterize photon migration in a settling suspension sample, numerical simulation based on a Monte-Carlo method was employed. For the simulation, the size and number of particles in a sample volume of 2035 mm^3 (diameter: 18 mm, thickness: 8 mm) were initially fixed to 20 μm and 221,011,174, respectively. The sample volume was horizontally divided into 8 layers with a thickness of 1 mm, and the number of particles in each layer was gradually varied to simulate particle settling, as shown in Table 3. In the table, the number of particles, population percentage, and inter-particle distance in each layer used for the Monte-Carlo simulation are summarized. Proceeding from case I to III, the degree of settling was increased.

Figure 8 shows the results of the Monte-Carlo simulation for distributed Raman photons in a simulated 8-layered sample for cases I, II, and III with application of TB (left column) and BT (right column) illumination. It was assumed that individual photons propagated independently through a suspension in a random walk-like fashion in three-dimensional space and incident radiation had a uniform intensity over the illumination area (1.77 mm^2 (diameter: 1.5 mm)). A detector was positioned opposite the laser illumination. Refractive indices used for aceclofenac and suspension solution were 1.639 and 1.467, respectively. Each dot indicates individually observed Raman photons. The wavy and straight arrows indicate the direction of laser illumination and gravitation (settling), respectively. The numbers at the left side of each simulation designate the serial number of sliced layers.

In the case of TB illumination, the photons are more densely populated in the layers opposite the illumination and their

Cite this: DOI: 10.1039/c0xx00000x

www.rsc.org/xxxxxx

ARTICLE TYPE

population is densest in layer 8. Since the laser initially illuminates a relatively less dense section of a sample such as layer 1, laser photons migrate through the sample to the opposite end with relatively less attenuation from scattering, thereby yielding a large number of Raman photons in layers 5-8. As settling proceeds further, such as from case I to III, the photon population in layers 5-8 becomes slightly decreased and more spread out. In particular, the photon population in layers 7-8, which neighbor the detector, were weaker resulting in a decrease of Raman intensity with settling as was observed experimentally (Fig.6 (a)). The decreased photon population in layers 7-8 for case III compared to cases I and II is attributed to the increased attenuation of laser photons by scattering in middle layers (such as layers 4 and 5) due to a more dense particle population.

The distribution of Raman photons in BT measurement is different from that in TB measurement. In case I, the photons are relatively more populated in the middle layers 4-6 and are moderately spread out in layers 1-3. Here, the detector is located behind layer 1. The greater photon attenuation by denser particles in the initial layers (layers 7-8) due to settling makes the photon population relatively greater in the middle rather than opposite layers (layers 1-2). From case I to III, the area of dense photon population in the middle moves down slightly due to increased scattering from the higher particle population in layers 7-8 during settling. Simultaneously, the Raman photon population in layers 1-2 decreases from case I to III, resulting in a decrease of the Raman signal with settling as was found experimentally (Fig. 6 (a)).

To examine the reproducibility of TB and BT measurements, the same number of laser photons was independently injected 10 times, and the RSDs of counted Raman photons at the detector were calculated for both cases. The RSDs of photon counting for cases I, II, and III were 0.16 %, 0.15 %, and 0.16 % for the TB measurement and 0.20 %, 0.24 %, and 0.23 % for the BT measurement, respectively. RSDs for the BT measurement were slightly higher in each case in accordance with the experimental observations as shown in Fig. 7 and Table 2. In the BT scheme, laser photons initially illuminate a denser section of the sample and generate a relatively larger amount of Raman photons that need to traverse through the denser section to reach the detector at the opposite end. During this course, uncertainty in photon migration through the sample increases, resulting in a relatively larger fluctuation in Raman intensity. In the TB measurement, the denser section generating more Raman photons is closer to the detector, and uncertainty in photon migration would decrease due to the shorter migration distance.

Influence of settling on accuracy for determination of aceclofenac concentration

Cite this: DOI: 10.1039/c0xx00000x

www.rsc.org/xxxxxx

ARTICLE TYPE

To examine the influence of settling on the accuracy of quantitative analysis, partial least squares (PLS) was employed to construct a calibration model incorporating the spectra of each sample collected at the 1st snapshot, and the constructed model was used to predict aceclofenac concentrations of the same samples during settling over one hour (from the 2nd to 50th snapshot). Normalized spectra in the 1800-1400 cm^{-1} range were used for the PLS analysis. For PLS modeling, the 73 % and 76 % aceclofenac sample in BT and TB measurements, respectively, were excluded since these were designated as outliers. In both cases, three factors were used for the modeling with 10-fold cross-validation. Acquired SECVs (Standard Error of Cross Validation) were 2.34 % and 2.49 % for the TB and BT measurements, respectively.

Figure 9 shows the variation of the standard error of prediction (SEP) for determination of aceclofenac concentration under ongoing particle settling employing the TB (blue) and BT (red) schemes. The SEP was obtained by predicting the spectra collected from the 2nd to 50th snapshot. The dashed line with the same color indicates the average SEP for each case. In both schemes, the SEP increased minutely; while, the fluctuation in the SEP along the snapshot was larger for the BT measurement. The standard deviation of 49 SEPs was 0.16 % and 0.21 % for the TB and BT measurements, respectively. The larger standard deviation in the BT measurement comes from the greater oscillation of aceclofenac intensity as found in Fig. 7 and the Monte-Carlo simulation.

Although the increase in error was insignificant, it apparently originates from the minute variation of spectral features during settling. To examine this spectral variation in more detail, the intensity ratio between aceclofenac at 1589 cm^{-1} and the suspension solution at 1665 cm^{-1} was examined. The intensity ratio could be a proper index that reflects consistency of sample representation. An unchanged ratio implies that the obtained Raman spectral features at any snapshot are quite representative of the suspension composition even with ongoing settling. Alternatively, a change in the intensity ratio would indicate a variation of compositional representation of a suspension sample.

Figure 10 shows the variation of the intensity ratio for the 1st-50th snapshot spectra for the 70 % (red), 100 % (blue), and 130 % (black) aceclofenac samples from TB (filled circles) and BT (open circles) measurements. On the bottom of the figure, the variations are individually magnified. The linear fitting lines (solid and dashed lines for TB and BT measurements, respectively) are also displayed. The intensity ratios generally remain steady over the one hour settling, while subtle changes are observed under magnification. The intensity ratios decrease and increase very slightly for the 70 % and 130 % aceclofenac samples, respectively, which demonstrate that the acquired Raman spectra during settling are not perfectly representative of the original suspension composition. The slopes of fitted lines from the BT measurements are

Cite this: DOI: 10.1039/c0xx00000x

www.rsc.org/xxxxxx

ARTICLE TYPE

minutely steeper compared to those from the TB measurements. Although axial illumination enables wide interaction with particles in a partially-settled sample, the varied inter-particle distances make it impossible to produce the same exact Raman features as under homogeneous conditions. Nonetheless, it is important to note that the magnitude of the spectral variation during settling obtained with the axial illumination scheme was very small and tolerable.

Figure 11 shows concentration correlation plots from the prediction of samples in the period of the 2nd - 50th snapshots using TB (a) and BT (b) measurements. The open and filled circles represent calibration and prediction data. The error bars correspond to the standard deviations of 49 predicted aceclofenac concentrations at each concentration. In both cases, the predicted concentrations are close to the ideal line, and the magnitudes of the error bars are small, indicating no substantial variation in the predicted values in the 2nd - 50th snapshots, although the TB measurement provides a more accurate determination of acelcofenac concentration.

Conclusions

We have first demonstrated an axial illumination scheme that can collect settling-tolerant Raman spectra for suspension samples. The TB scheme allowing axial laser radiation along the same direction as settling was more effective in acquiring more reproducible Raman spectra of aceclofenac suspensions. In a partially settled suspension sample, particle concentrations in a given area are never the same throughout the suspension sample, thus covering an entire sample for Raman spectral acquisition is critically necessary for accurate compositional representation. We are currently evaluating the TB scheme as a potential PAT (Process Analytical Technology)[17] tool for non-destructive analysis of suspension samples in several types of pharmaceutical containers such as gel capsules.

Acknowledgements

This research was supported by Basic Science Research Program through the National Research Foundation of Korea (NRF) funded by the Ministry of Education, Science and Technology (2012R1A1B3003965). This work was supported by NRF (National Research Foundation of Korea) Grant funded by the Korean Government (NRF-2011-0008638-Global Ph.D. Fellowship Program).

Notes and references

Cite this: DOI: 10.1039/c0xx00000x

www.rsc.org/xxxxxx

ARTICLE TYPE

[a] *Department of Chemistry, College of Natural Sciences, Hanyang University, Seoul, 133-791, Korea. Fax: 82-2-2299-0762; Tel: 82-2-2220-0937; E-mail: hoeil@hanyang.ac.kr*

[b] *Chong Kun Dang Pharm., Cheonan-si, Chungcheongnam-do, Korea*

1 M.T. Islam, N. Rodriguez-Hornedo, S. Ciotti and C. Ackermann, *Pharmaceutical Research,* 2004, **21**, 1844.

2 T.R.M. De Beer, G.J. Vergote, W.R.G. Baeyens, J.P. Remon, C. Vervaet and F. Verpoort, *European Journal of Pharmaceutical Sciences*, 2004, **23**, 355.

3 T.R.M. De Beer, W.R.G. Baeyens, J. Ouyang, C. Vervaet and J.P. Remon, *Analyst*, 2006, **131**, 1137.

4 S.C. Park, M. Kim, J. Noh, H. Chung, Y. Woo, J. Lee and M.S. Kemper, *Analytica Chimica Acta*, 2007, **593**, 46.

5 T.R.M. De Beer, W.R.G. Baeyens, A. Vermeire, D. Broes, J.P. Remon and C. Vervaet, *Analytica Chimica Acta*, 2007, **589**, 192.

6 Y. Pu, J.P. Medendorp and C.R. Yonzon, *J. Raman Spectrosc*., 2011, **42**, 1994.

7 C.S. Yong, Y.-K. Oh, K.H. Lee, S.-M. Park, Y.-J. Park, Y.S. Gil, C.H. Yu, B.-K. Yoo, J.S. Woo, J.O. Kim, J.-D. Rhee, C.-K. Kim and H.-G. Choi, *International Journal of Pharmaceutics*, 2005, **302**, 78.

8 M. Kim, H. Chung, Y. Woo and M. Kemper, *Analytica Chimica Acta*, 2006, **579**, 209.

9 F.F.M. De Mul, M.H. Koelink, M.L. Kok, P.J. Harmsma, J. Greve, R. Graaff and J.G. Aarnoudse, *Appl. Opt.*, 1995, **34**, 6595.

10 F.F.M. De Mul, in *Handbook of Coherent Domain Optical Methods, Biomedical Diagnostics, Environment and Material Science*, ed. V.V. Tuchin, Kluwer Publishers, Boston, 2004.

11 N.-S. Cheng, *J. Hydraul. Eng.*, 1997, **123**, 728.

12 J.P. Coakley and J.P.M. Syvitski, in *Principles, Methods, and Application of Particle Size Analysis*, ed. J.P.M. Syvitski, Cambridge University Press, Cambridge, 1991.

13 T.J. McGhee and E.W. Steel, in *Water supply and sewerage, McGraw-Hill series in water resources and environmental engineering*, McGraw-Hill, New York, 6th edn., 1991.

14 S. Koo, *Journal of Industrial and Engineering Chemistry*, 2009, **15,** 45.

15 E. Barnea and J. Mizrahi, *Chem. Eng. J.*, 1973, **5**, 171.

Cite this: DOI: 10.1039/c0xx00000x

www.rsc.org/xxxxxx

ARTICLE TYPE

16 P.A. Vesilind, J.J. Peirce and R.F. Weiner, in *Environmental Engineering*, Butterworth Heinemann, 3rd edn., 1994.

17 A.S. Rathore, R. Bhambure and V. Ghare, *Anal. Bioanal. Chem.*, 2010, **398**, 137.

Tables :

Table 1. Percent intensity variation of the aceclofenac band during settling for the 70 %, 100 %, and 130 % samples with upper and lower sample illumination

70 % Aceclofenac		100 % Aceclofenac		130 % Aceclofenac	
Upper	Lower	Upper	Lower	Upper	Lower
62.1 %	117.9 %	92.8 %	103.4 %	100.3 %	100.6 %

Cite this: DOI: 10.1039/c0xx00000x

www.rsc.org/xxxxxx

ARTICLE TYPE

Table 2. Calculated percent variation of the aceclofenac band at the 50th snapshot relative to the 1st snapshot from the TB and BT schemes for the 70 %, 100 %, and 130 % samples. The numbers in parentheses indicate the RSD of 50 intensity values (Fig. 7) for each sample.

70 % Aceclofenac		100 % Aceclofenac		130 % Aceclofenac	
TB	BT	TB	BT	TB	BT
100.1 % (0.19 %)	99.6 % (0.26 %)	100.2 % (0.26 %)	100.1 % (0.32 %)	100.4 % (0.25 %)	100.5 % (0.28 %)

Cite this: DOI: 10.1039/c0xx00000x

www.rsc.org/xxxxxx

ARTICLE TYPE

Table 3. Number of particles, population percentage, and inter-particle distance in each layer used for the Monte-Carlo simulation

	Layer	Number of particles	Percentage in population (%)	Inter-particle distance (μm)
Case I	1	19,326,105	8.7	13.6
	2	21,258,716	9.6	12.9
	3	23,384,587	10.6	12.1
	4	25,723,046	11.6	11.5
	5	28,295,350	12.8	10.8
	6	31,124,885	14.1	10.1
	7	34,237,374	15.5	9.5
	8	37,661,111	17.0	8.9
Case II	1	13,395,360	6.1	16.7
	2	16,074,432	7.3	15.1
	3	19,289,318	8.7	13.6
	4	23,147,182	10.5	12.2
	5	27,776,618	12.6	10.9
	6	33,331,941	15.1	9.7
	7	39,998,330	18.1	8.5
	8	47,997,996	21.7	7.4
Case III	1	9,263,729	4.2	20.2
	2	12,042,847	5.4	17.6
	3	15,655,702	7.1	15.3
	4	20,352,412	9.2	13.2
	5	26,458,136	12.0	11.3
	6	34,395,576	15.6	9.5
	7	44,714,249	20.2	7.8
	8	58,128,524	26.3	6.3

Cite this: DOI: 10.1039/c0xx00000x

www.rsc.org/xxxxxx

ARTICLE TYPE

Figures :

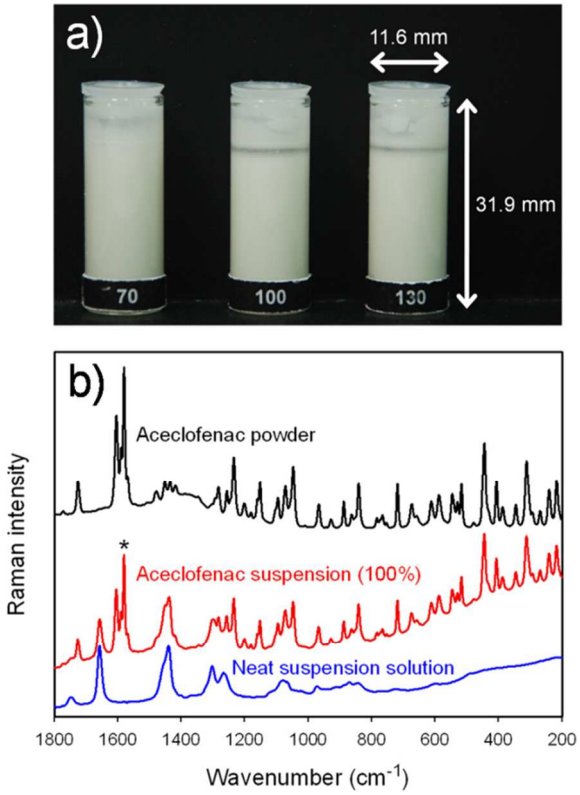

Fig. 1 (a) Photographs of 70 %, 100 %, and 130 % aceclofenac suspensions in glass vials. (b) Raman spectra of aceclofenac powder (black), aceclofenac suspension (red), and neat suspension solution (blue). The asterisk indicates the most intense aceclofenac band at 1589 cm^{-1}.

Cite this: DOI: 10.1039/c0xx00000x

www.rsc.org/xxxxxx

ARTICLE TYPE

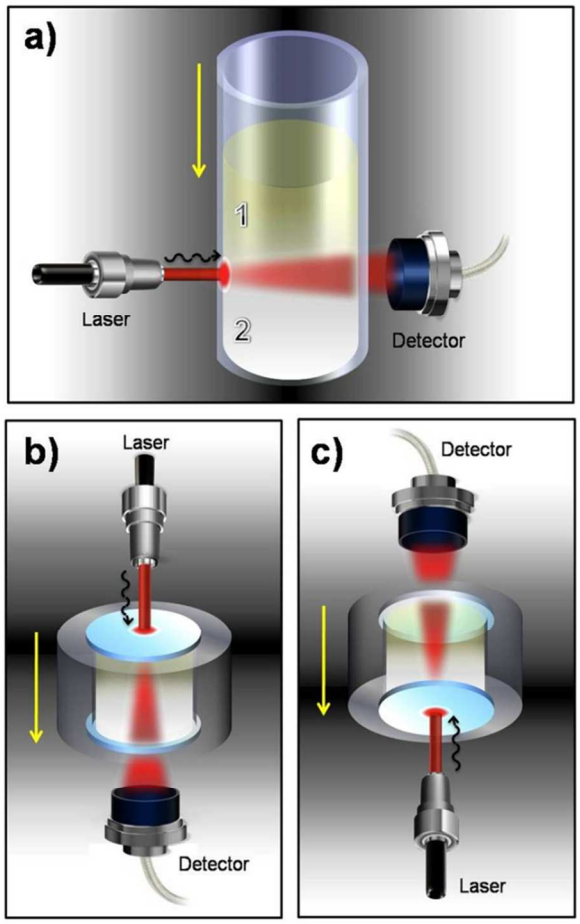

Fig. 2 Graphical depiction of the perpendicular (a), TB axial (b), and BT axial (c) illumination schemes for collection of transmission Raman spectra of a suspension sample. Wavy and straight arrows indicate the direction of laser illumination and particle settling (gravity), respectively.

Cite this: DOI: 10.1039/c0xx00000x

www.rsc.org/xxxxxx

ARTICLE TYPE

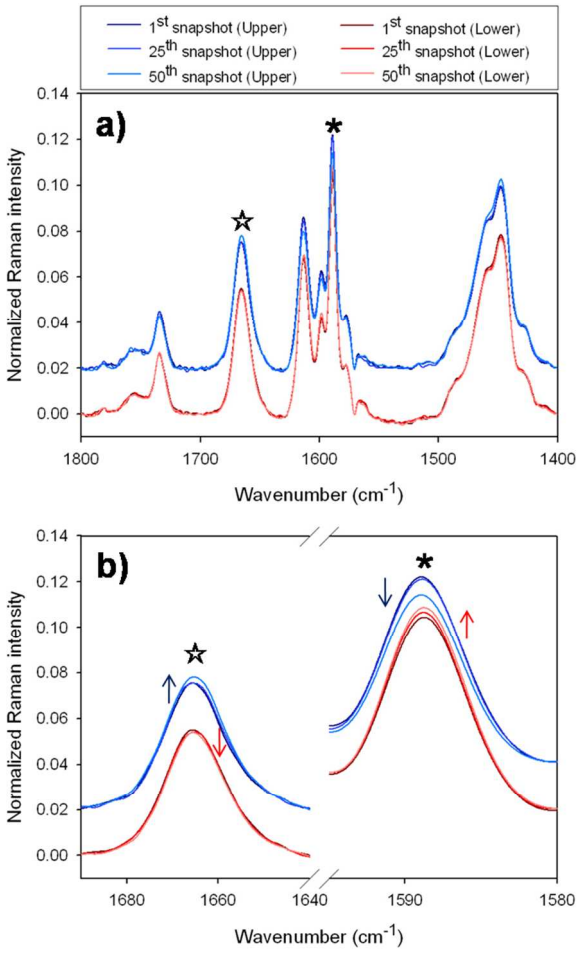

Fig. 3 (a) Normalized Raman spectra of the 100 % aceclofenac sample collected at the 1st, 25th, and 50th snapshots with perpendicular laser illumination of the upper (blue) and lower (red) areas of the sample (a). Major aceclofenac and suspension solution peaks at 1589 (marked by asterisk) and 1665 cm^{-1} (marked by star), respectively, are highlighted (b). Arrows indicate the direction of intensity change with particle settling.

Cite this: DOI: 10.1039/c0xx00000x

www.rsc.org/xxxxxx

ARTICLE TYPE

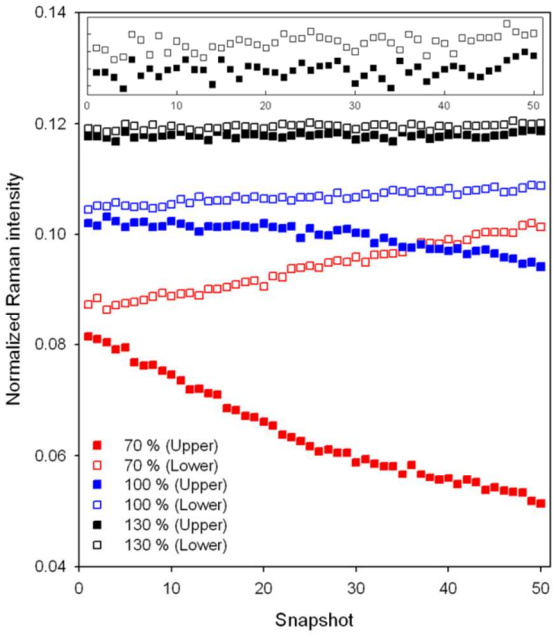

Fig. 4 Intensity variation of the aceclofenac band during one hour settling obtained from the 70 % (red), 100 % (blue) and 130 % (black) samples for upper (filled square) or lower (open square) sample illumination. The intensity variation for the 130 % aceclofenac sample is magnified in the inset.

Cite this: DOI: 10.1039/c0xx00000x

www.rsc.org/xxxxxx

ARTICLE TYPE

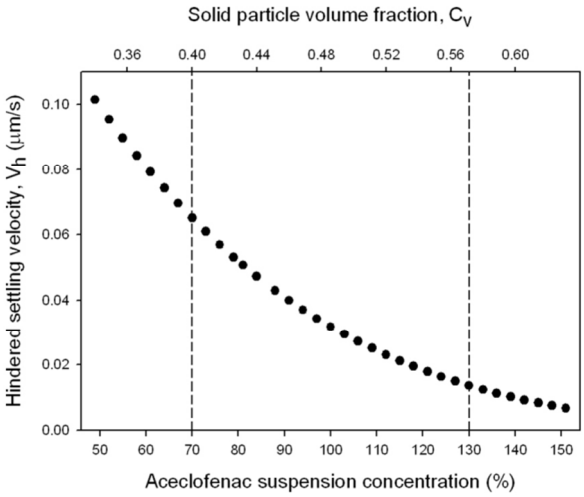

Fig. 5 The variation of hindered settling velocity (V_h) as a function of solid volume fraction (C_v). C_v of 0.40 and 0.57 corresponds to a aceclofenac concentration of 70 % and 130 %, respectively, as indicated by the dashed lines.

Cite this: DOI: 10.1039/c0xx00000x

www.rsc.org/xxxxxx

ARTICLE TYPE

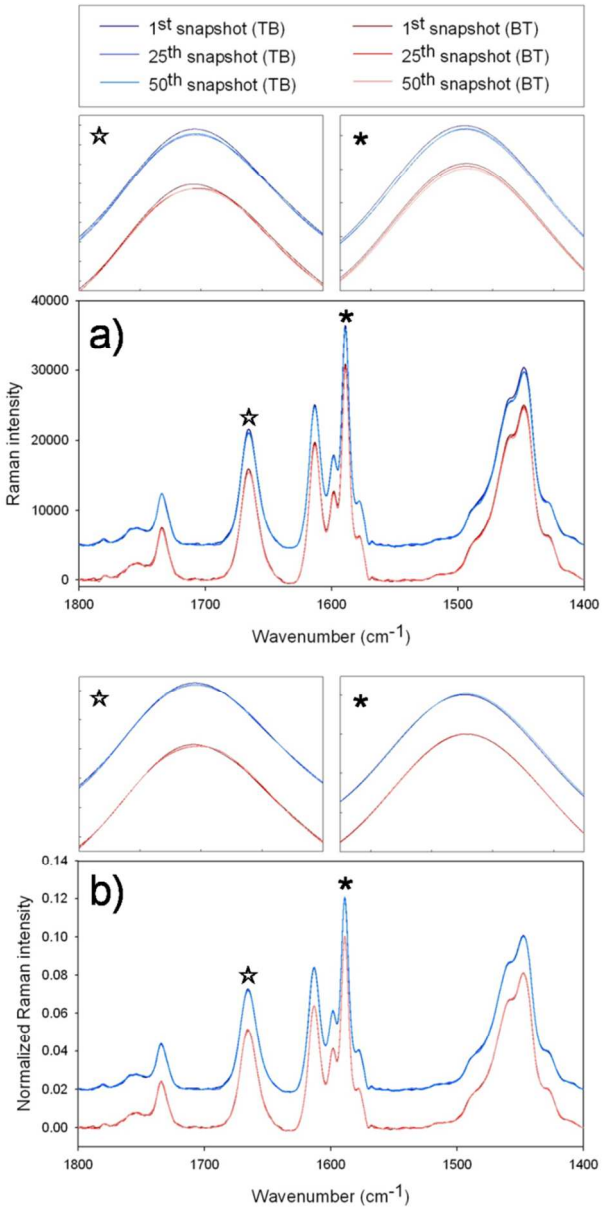

Fig. 6 The baseline-corrected Raman spectra of the 100 % aceclofenac sample in the 1800-1400 cm^{-1} range collected by TB (blue) and BT (red) schemes (a) and the corresponding normalized Raman spectra (b). Both aceclofenac (asterisk) and neat suspension (star) bands are magnified on the top the corresponding figure.

Cite this: DOI: 10.1039/c0xx00000x

www.rsc.org/xxxxxx

ARTICLE TYPE

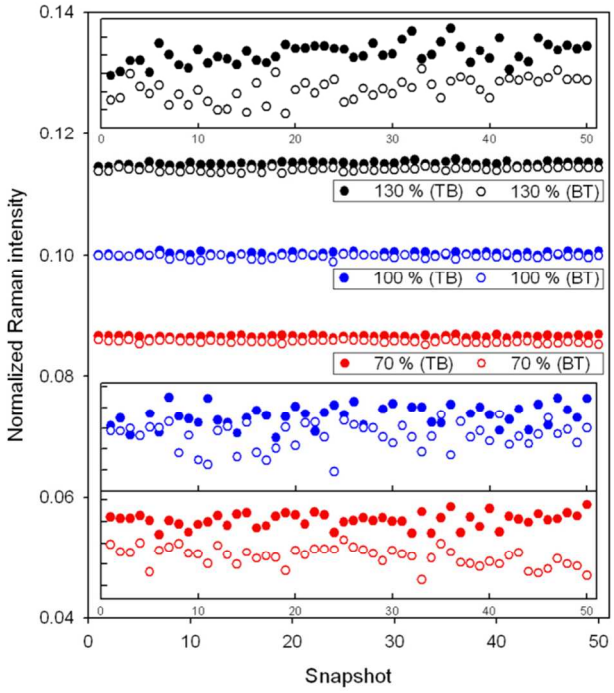

Fig. 7 The intensity variation of the normalized aceclofenac band during one hour settling of the 70 % (red), 100 % (blue) and 130 % (black) samples from TB (filled circle) and BT (open circle) measurements. For detailed examination, the intensity variations are magnified in the insets.

Cite this: DOI: 10.1039/c0xx00000x

www.rsc.org/xxxxxx

ARTICLE TYPE

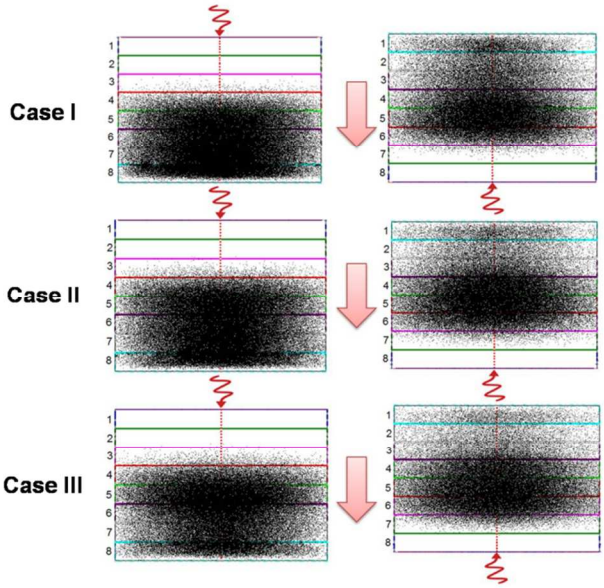

Fig. 8 The results of a Monte-Carlo simulation showing the distribution of Raman photons in a simulated 8 layered sample for cases I, II, and III with application of TB (left column) and BT (right column) illumination.

Cite this: DOI: 10.1039/c0xx00000x

www.rsc.org/xxxxxx

ARTICLE TYPE

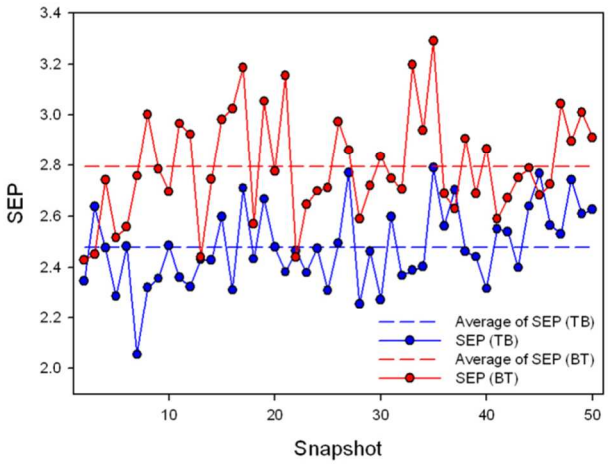

Fig. 9 Variation of the standard error of prediction (SEP) for the determination of aceclofenac concentration under ongoing particle settling employing the TB (blue) and BT (red) schemes. The dashed line with the same color indicates the average SEP.

Cite this: DOI: 10.1039/c0xx00000x

www.rsc.org/xxxxxx

ARTICLE TYPE

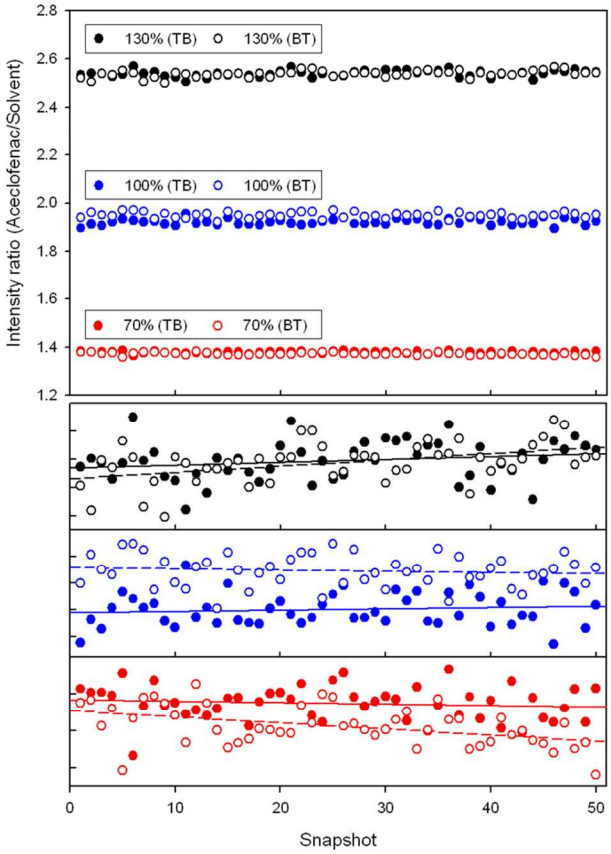

Fig. 10 Variation of the intensity ratio in the 1st-50th snapshot spectra for the 70 % (red), 100 % (blue), and 130 % (black) aceclofenac samples for TB (filled circles) and BT (open circles) measurements. Variations are individually magnified on the bottom of the figure.

Cite this: DOI: 10.1039/c0xx00000x

www.rsc.org/xxxxxx

ARTICLE TYPE

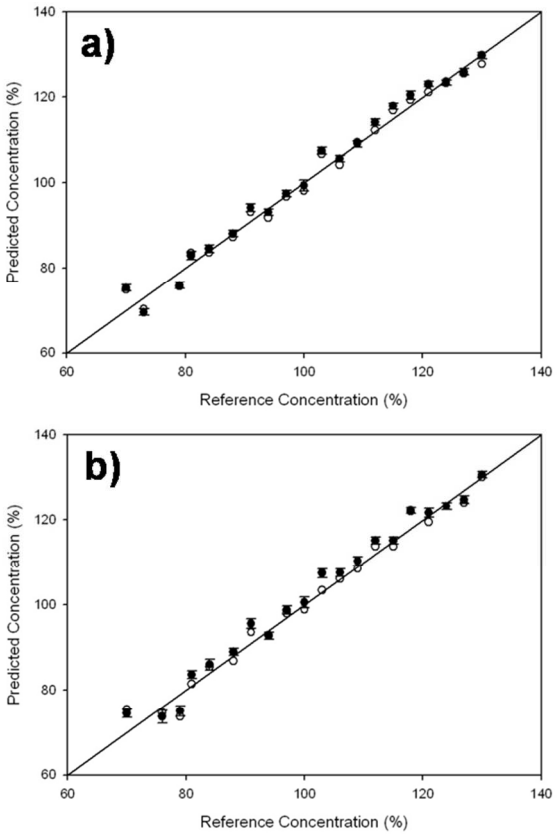

Fig. 11 Concentration correlation plots resulting from the prediction of samples in the period of the 2nd - 50th snapshot using the TB (a) and BT (b) schemes. Open and filled circles represent calibration and prediction data. The error bars correspond to the standard deviations of 49 predicted aceclofenac concentrations during the one hour settling.

Cite this: DOI: 10.1039/c0xx00000x

www.rsc.org/xxxxxx

ARTICLE TYPE

TOC only